# EFFECT OF HIGH-TEMPERATURE HEATING OF BIMETALLIC STEEL BILLETS

**A. N. Tikhonov, V. D. Kal'ner, I. N. Shklyarov, V. B. Glasko, N. I. Kulik, and V. V. Akimenko**

UDC 536.24.02

*A mathematical model of high-temperature induction heating of a two-layer bimetallic cylindrical specimen with an allowance for the effect of thermoelastoplastic loading has been developed on the basis of the inverse problem method. The results of a mathematical experiment on determining the optimum heating conditions connected with abrupt changes in the inductor's dynamic parameters are provided.*

1. Bimetallic or trimetallic billets and finished parts made of alloys with different physicochemical characteristics are finding application to an ever increasing extent in various branches of the national economy as one of the most economic methods of ensuring the required quality of parts.

A constraining factor in developing specific technologies for processing actual bimetallic materials is the lack of practical ways of estimating the contact stresses and temperature fields at the interface between actual parts and, as a consequence, the inevitable use of prolonged, slow heating in special protective atmospheres (for instance, an oxidizing atmosphere). The latter complicates production and raises costs to a considerable extent.

A two-stage procedure can be used for reducing the time of preliminary induction heating of such specimens: As the material surface loses its magnetic properties (passage through the Curie point), possibly with a certain lag, the current amplitude I increases in the inductor simultaneously with an increase in its frequency f [1]. This procedure also ensures a uniform temperature distribution over the specimen's cross section with the allowable temperature drop in the external layer throughout the time interval. The reduction in the heating time resulting from this makes it possible to reduce the processing costs and steel wastage due to oxidation.

We are concerned with approbation of the method for calculating the temperature and elastoplastic fields in a bimetallic specimen with the aim of determining the optimum conditions of heating control. The problem of determining the inductor current with respect to the experimentally assigned temperature conditions at the specimen's surface is solved first. The solution of such a problem, which belongs to the class of inverse problems [2, 3], makes it possible to realize a mathematical experiment in a wide range of control parameters without complicating the model. In order to solve this problem, we shall modify somewhat the special regulating algorithm proposed in [4] for calculating the control in heating monometallic parts.

2. In stating the problem of determining the temperature field in the specimen T(r, t) (the cross section is shown in Fig. 1), we shall consider, in contrast to [4], the radiative heat exchange at the outside surface of the cylinder, which, as before, is assumed to have an infinite extent.

Under these assumptions and for the assigned induction current parameters, the mathematical model of the heating of a bimetallic specimen is described by the following conditions:

$$A(T,\ H) \equiv \frac{1}{r}\frac{\partial}{\partial r}\left(r\lambda_s(T)\ \frac{\partial T_s}{\partial r}\right) + q(T,\ H) - c_s(T)\gamma_s(T)\ \frac{\partial T_s}{\partial t} = 0 \tag{1}$$

$$(0 < r < R_2,\ 0 < t \leqslant \bar{t});$$

$$\left.\frac{\partial T_1}{\partial r}\right|_{r=0} = 0,$$

$$T_1|_{r=R_1} = T_2|_{r=R_1},\ \lambda_1 \left.\frac{\partial T_1}{\partial r}\right|_{r=R_1} = \lambda_2 \left.\frac{\partial T_2}{\partial r}\right|_{r=R_1}, \tag{2}$$

M. V. Lomonosov Moscow State University. Translated from Inzhenerno-Fizicheskii Zhurnal, Vol. 58, No. 3, pp. 392-401, March, 1990. Original article submitted March 6, 1989.

0022-0841/90/5803-0281$12.50  

$$-\lambda_2(T)\frac{\partial T_2}{\partial r}\bigg|_{r=R_2}=\hat{h}(T_2-T^0)|_{r=R_2}+\hat{\sigma}\hat{\chi}(T_2^4-T^{0^4})_k|_{r=R_2};\qquad(3)$$

$$T_s|_{t=0}=T^0.$$

Here and below, the values s = 1, 2 pertain to the characteristics of metals I and II, respectively, $\lambda$ is the thermal conductivity, c is the specific heat, $\gamma$ is the density, $\hat{h}$ is the coefficient of heat transfer at the surface, $\hat{\sigma}$ is the Stefan—Boltzmann constant (equal to $5.67\cdot10^{-8}$ W/(m$^2$·K$^4$)), $\hat{\chi}$ is the degree of blackness of the solid (equal to 0.8), q is the heat source, and $\overline{t}$ is the over-all time of induction heating.

The density of heat sources $q = 1/2\ \rho_s(T)\ |\partial H_s/\partial r|^2$ is calculated by solving the Maxwell equations and, correspondingly, the following boundary-value problem:

$$B(T,\ H)\equiv\frac{1}{r}\frac{\partial}{\partial r}\left(r\rho_s(T)\frac{\partial H_s}{\partial r}\right)+i\omega\mu_s(T)H_s-\frac{\partial}{\partial t}(\mu_s(T)H_s)=0\qquad(4)$$

$$(0<r<R_2,\ 0<t\leqslant\overline{t});$$

$$\frac{\partial H_1}{\partial r}\bigg|_{r=0}=0,\qquad(5)$$

$$H_1|_{r=R_1}=H_2|_{r=R_1},\ \rho_1\frac{\partial H_1}{\partial r}\bigg|_{r=R_1}=\rho_2\frac{\partial H_2}{\partial r}\bigg|_{r=R_1},\qquad(6)$$

$$H_2|_{r=R_2}=nI;$$

$$H_s|_{t=0}=0.$$

Here, H(r, t) is the strength of the magnetic field, $\rho$ is the resistivity, n is the number of inductor windings per unit length (1/mm), I is the inductor current, $\mu$ is the permeability, f is the current frequency: $\omega = 2\pi f$ ($f = f_1$, $T(R_2) < T_2^K$; $f = f_2$, $T(R_2) \geq T_2^K$), and $T_2^K$ is the temperature at the Curie point of material II.

For the assigned thermal and electromagnetic characteristics of the materials ($\lambda = \lambda(T)$, $c = c(T)$, $\gamma = \gamma(T)$, $\mu = \mu(T)$, $\rho = \rho(T)$) and for each set of the control parameters (I(t), $f_1$, $f_2$), the nonlinear system of equations (1)-(6) is solved by means of the iteration difference scheme, which has an accuracy of the order of $O(\Delta r^2 + \Delta t)$ and is implicit with respect to time [5].

The modification of the trial-and-error method proposed in [6] was used in the program developed for our inhomogeneous medium. On the whole, such a program performs the function of the "sensing element" for the temperature field for the assigned parameters which control the operating conditions.

3. In stating the inverse problem, we consider that the values of $f_1$ and $f_2$ are assigned in advance, which corresponds to the use of standard ac current sources. The opportunities provided by deviation from the standard can always be determined by direct variation of these parameters. Then, the object of the inverse problem is to determine the function I = I(t) along with the temperature field.

For the statement of the problem, it is sufficient to assign the additional surface temperature of the specimen $\tilde{\varphi}(t)$ and the tolerance $\delta$ for the deviation from this temperature [4]:

$$F(I)=\int_0^{\overline{t}}[T/R_2,\ t)-\tilde{\varphi}(t)]^2\,dt\leqslant\delta^2.\qquad(7)$$

Here, $\tilde{\varphi}(t)$ is the temperature determined experimentally, and $T(R_2, t)$, which is calculated from conditions (1)-(6), is the surface temperature, which thereby constitutes the functional of I(t): $T(R_2, t) \equiv T[R_2, t, I(t)]$.

As additional information on the quantity to be determined that would enhance the stability of the approximation, we use the assumption that the I(t) function is everywhere "continuous," with the exception of a small time interval corresponding to the neighborhood of the Curie point (for material II), and the condition $I(t) \geq 0$ for any t.

The realization of both these sets of conditions can be secured within the framework of the step-by-step algorithm, in a manner similar to that used in [4], over any time segment $[t_j, t_{j-1}]$:

$$I_j=\arg\min(I-I_{j-1})^2,$$

$$I\in X_j\equiv\{I:I\geqslant0,\ F_j(I)\leqslant\delta_j^2\}\qquad(8)$$

$$(j=0,\ 1,\ \ldots,\ M),$$

$$I_0=0,$$

where

$$\delta_j^2=\delta^2/M,\ F_j(I)\equiv\int_{t_{j-1}}^{t_j}[T(R_2,\ t)-\tilde{\varphi}(t)]^2dt,\ t_j=j\Delta t,\ \Delta t=\overline{t}/M.$$

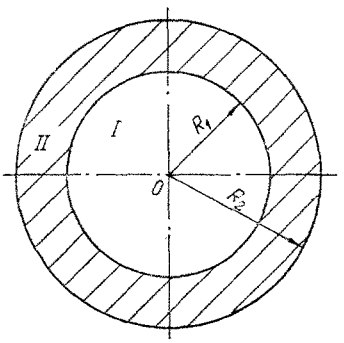


Fig. 1. Cross section of the bimetallic specimen.

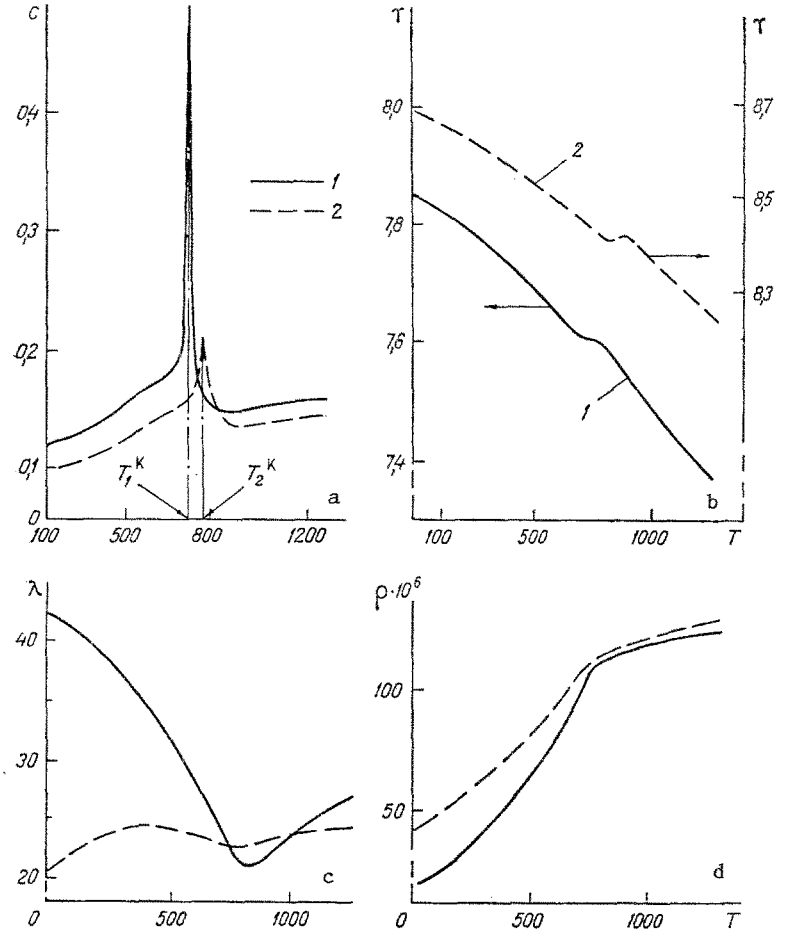


Fig. 2. Physical characteristics of the materials of specimens. a) Specific heat; b) density; c) thermal conductivity; d) resistivity; 1) U8 steel, $T_2^K$ = 730°C; 2) R18 steel, $T_2^K$ = 780°C (c, cal(g·°C); $\gamma$, g/cm$^3$; $\lambda$, kcal/m.p.°C; $\rho$, Ω·cm).

For the realization of (8) in practice, it is sufficient to minimize, as in [4], the "local misclosure" functional $F_j(I)$ over each following time segment, for instance, by means of the Newton—Gauss method [7], using the already found value $I_{j-1}$ as the initial approximation.

The condition for $I_j$ to be nonnegative can be realized by using the "projection" method: In our problem, if a negative value is obtained, it is sufficient to substitute zero for it in the next time segment.

In view of the connectedness of problems (1)-(6), the resultant temperature field is calculated "simultaneously" with the control current. We have solved this inverse problem for a bimetallic specimen consisting of materials similar

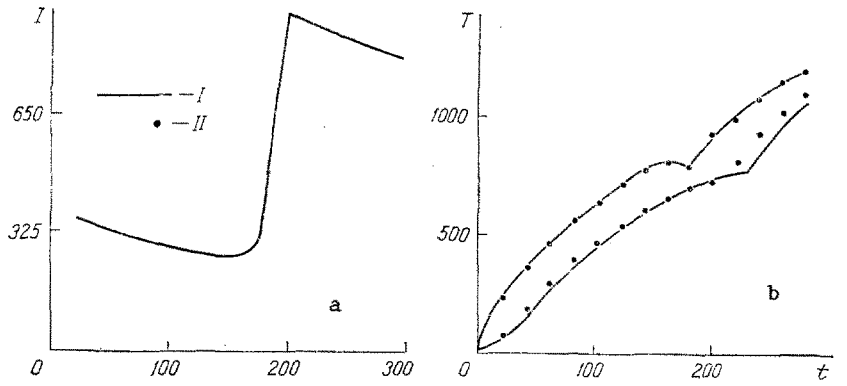


Fig. 3. Recovery of the control current with respect to experimental data. a) Current as a function of time; b) temperature field at the surface (1) and the axis (2) of the specimen. I) Experimental data; II) calculations based on the current from (a); $R_2$ = 32.5 mm; $R_1$ = 27.5 mm; $f_1$ = 2400 Hz; $f_2$ = 10,000 Hz; I is given in amperes; t is given in seconds.

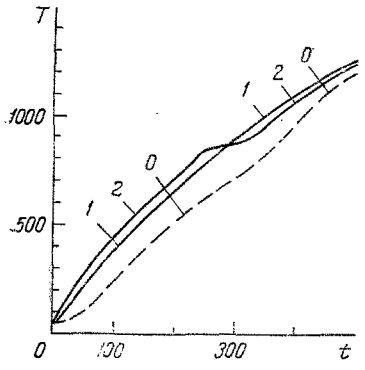


Fig. 4

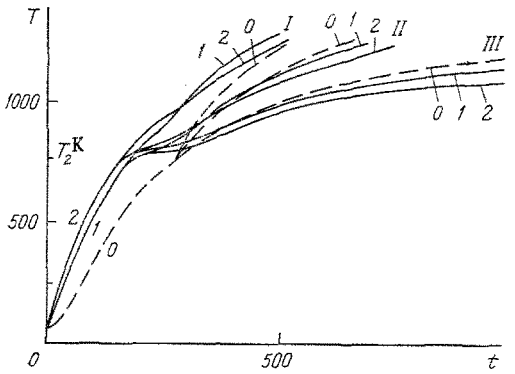


Fig. 5

Fig. 4. Temperature field characteristics: temperature at the surface, r = $R_2$ (2); at the interface, r = $R_1$ (1); at the specimen's axis, r = 0 (0); $R_2$ = 50 mm; $R_1$ = 40 mm; $f_1$ = 50 Hz; $f_2$ = 1000 Hz; $I_1$ = 850 A; $I_2$ = 1350 A.

Fig. 5. Dependences of the temperature field characteristics on the inductor current frequency (temperature at the surface, r = $R_2$ (2); at the interface, r = $R_1$ (1); at the specimen's axis, r = 0 (0)); $R_2$ = 50 mm; $R_1$ = 40 mm; $I_1$ = $I_2$ 1222 A; $f_1$ = 50 Hz; $f_2$ = 2500 Hz (I); 1000 Hz (II); 500 Hz (III).

to those used in practice: an outside layer made of R18 steel (material II in Fig. 1) and a core consisting of U8 steel (material I). The physical characteristics of these materials are represented in Fig. 2.

In the experiment performed under laboratory conditions at Likhachev Automobile Plant (ZIL), the geometric parameters of the specimen were the following: $R_1$ = 27.5 mm; $R_2$ = 32.5 mm. The specimen was heated by current at the frequency $f_1$ = 2400 Hz over a period of 0-170 sec, followed by a 10-sec pause, connected with transferring the specimen to another inductor. The duration of heating in the latter was equal to 90 sec at the current frequency $f_2$ = 10,000 Hz. During the heating process, the temperature fields at the surface of the specimen, inside it, and at its axis were measured by means of thermocouples.

These data were actually used as indirect information on the current behavior in time for recovery of the current within the framework of the above statement of the inverse problem. The result of its solution is given in Fig. 3a. Evidently, the piecewise continuous curve that has been chosen according to the algorithm from the set of continuous functions approximates the actual distribution, which comprises the pause. The points in Fig. 3b represent the temperature values calculated with respect to the current determined, which are compared with the experimental data.

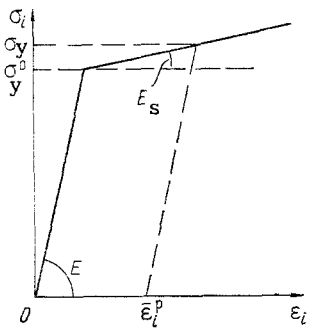


Fig. 6. Loading model with linear strain hardening: $\sigma_y$) instantaneous yield point; $\varepsilon^{p_i}$) cumulative plastic deformation; E) elasticity (Young) modulus; $E_s$) shear modulus in the plasticity region.

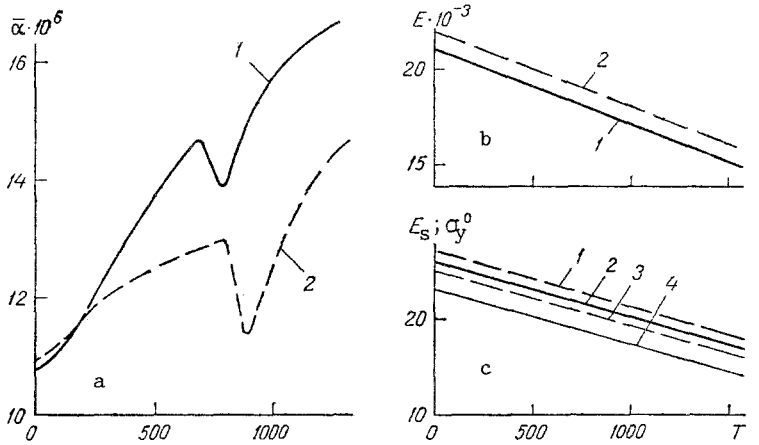


Fig. 7. Thermomechanical characteristics of the materials. a) Linear expansion coefficient; b) elasticity modulus: 1) U8 steel, 2) R18 steel; c) shear modulus: 1) R18 steel, 2) U8 steel; yield point: 3) R18 steel, 4) U8 steel; $\bar{\alpha}$, 1/deg C; E, $E_s$, and $\sigma_y^0$, kgf/mm$^2$.

The satisfactory agreement between the temperature fields confirms the efficiency of our algorithm. The greater difference between the fields at r = 0 can be explained by the discrepancy between the steel parameters in the core determined theoretically and in experiments.

4. The solution of the inverse problem of determining the control current with respect to data from indirect observations not only serves for checking whether the model adopted reflects adequately the actual process, but also provides an idea of the character and level of the control current even if its behavior is not known beforehand. With an accuracy sufficient for practical purposes and in correspondence with actual conditions, this behavior can be compared with the piecewise continuous function $I(t) = I_1(\psi(t)-\psi(t-\tau_k) + I_2\psi(t-\tau_k))$, where $I_1$ and $I_2$ are constant values, $\tau_k = \tau_k(T^K)$ is the instant of time at which the surface temperature passes through the Curie point, and $\psi(t)$ is the Heaviside function (0 if $t \leq 0$; 1 if $t > 0$). In this, the order of magnitude of $I_1$ and $I_2$ is known.

This makes it possible to solve by means of a computer the problem of optimum control of the technological process of high-temperature heating of a bimetal within a realistic range of the control parameters: $\mathbf{p} = \{I_1, I_2; f_1, f_2\} \in P$.

In our case, the optimum-control problem consists in determining the parameter **p** so that the heating to the assigned temperature $\hat{T}$ (~1200°C) is accomplished in the minimum time under the condition that the temperature drop in the outside layer of the bimetal ($\delta$ = 50°C) does not exceed the assigned value.

It is assumed that, with such a temperature drop, the thermal stress field in this region does not produce fractures or residual effects. As will be shown in section 5, this assumption admits of verification in a mathematical experiment.

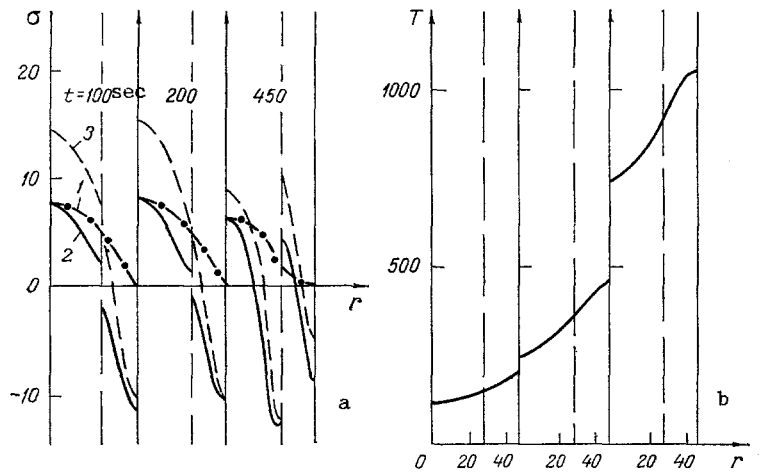


Fig. 8. Distribution of the process characteristics in time at different instants of time: a) stress tensor components: 1) $\sigma_{rr}$; 2) $\sigma_{\theta\theta}$; 3)$\sigma_{zz}$; b) temperature; $R_2$ = 50 mm; $R_1$ = 30 mm; $f_1$ = 50 Hz; $f_2$ = 2500 Hz; $I_1$ = 625 A; $I_2$ = 1125 A; r is given in millimeters.

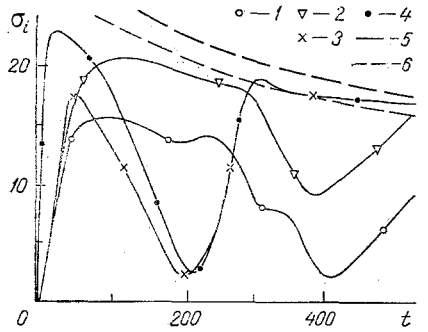


Fig. 9. Distribution of the stress intensity in time for the optimum control variant (see Fig. 4). 1) At r = 0 (material I); 2) at r = $R_1$ (material I); 3) at r = $R_1$ (material II); 4) at r = $R_2$ (material II); yield point: 5) material I; 6) material II.

In view of the fact that a small, discrete set of frequencies is used in practice, then, for the sake of economy, we naturally consider the problem of optimization with respect to $\hat{I} = \{I_1, I_2\}$ for a fixed pair $\hat{f} = \{f_1, f_2\}$. The temperature field then depends functionally on $\hat{I}$: $T = T[(r, t, \hat{I}]$.

We introduce the following functional: $\Phi_1(\hat{I}) \equiv \{T[R_2, t, \hat{I}] - T[R_1, t, \hat{I}]\}^2$ and define the total heating time $\hat{t} = \hat{t}(\hat{I})$ assigning by the condition $T[R_2, \hat{t}, \hat{I}] = \hat{T}$. Then, the optimum control problem stated above is formulated for any $\hat{f}$ in the following manner:

$$\hat{\tau} = \arg\inf \hat{t}(\hat{p}),\ \hat{p} \in \{(\hat{I},\ \hat{f}) \in P,\ \Phi_t(\hat{I}) \leqslant \hat{\delta}^2,\ t \in [0,\ \hat{t}]\}. \tag{9}$$

As a possible algorithm for solving this problem, we can obtain, by using a previously assigned grid, a sample of $\hat{t}$ values from among those for which $\inf_{(\hat{I}, \hat{f}) \in P} \Phi_t(\hat{I}) \leq \hat{\delta}^2$. The solution of the $\inf \Phi_t(\hat{I})$ problem (similar to the problem of the quasi-solution [2, 3]) does not involve fundamental difficulties.

Figure 4 shows the temperature field characteristics for one set of geometric parameters and $\hat{f}$ under optimum conditions. The heating duration is equal to $\overline{t}$ = 520 sec for this variant. It is evident that control of this type is efficient, and the temperature drop in the outside layer is reduced even more after the current is switched.

The temperature field characteristics under optimum operating conditions for a large specimen are shown in Fig. 5 as functions of the $f_2$ value ($f_1$ = 50 Hz). It is evident that the optimum time increases with a reduction in the frequency difference. Thus, if suitable technological means are available the choice of the current frequency after switching can be used as a factor in process optimization.

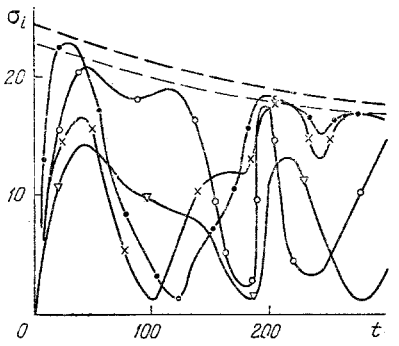


Fig. 10. Characteristics of the stress field in the experimental variant (see Fig. 3). The notation is the same as in Fig. 9.

The above variants also indicate that, under optimum conditions, the temperature drop along the radius, $0 < r < R_2$, is not too large either, and the temperature field approaches equilibrium after the heating ends.

5. We shall now turn to control of the stress field corresponding to the optimum control with respect to the temperature field. This control can be realized as a result of a direct mathematical experiment for the operating parameters chosen above within the framework of any model of the thermomechanical state of a material.

Generally speaking, transition of a metal to the plasticity region must not be neglected in high-temperature heating. On the other hand, neglecting the inverse effect of the stress field on the temperature field, we can consider the thermomechanical problem in the quasi-stationary approximation. In this case, the time and, correspondingly, the temperature as a function of the radius, determined by system (1)-(6), constitute functional parameters of the thermomechanical equations.

The stress fields which we calculated for the loading model with linear strain hardening [8] are represented in Fig. 6. The thermomechanical parameters of the materials in the specimens, including the instantaneous yield point and the tangent modulus in the plasticity region [9, 10], are shown in Fig. 7.

The fields of stresses ($\sigma_{ij}$, i, j = r, $\theta$, z), strain ($\varepsilon_{ij}$), and radial displacements ($u_r$) which depend only on r and t are described in each layer by the following system of equations, where $d\sigma_{ij}$, etc. are increments of the initial quantities in time:

$$\frac{\partial}{\partial r}(d\sigma_{rr}) + \frac{d\sigma_{rr} - d\sigma_{\theta\theta}}{r} = 0, \tag{10}$$

$$d\varepsilon_{ij} = d\varepsilon_{ij}^E + d\varepsilon_{ij}^P \tag{11}$$

(where the superscript E pertains to elastic, and the superscript P to plastic, strain),

$$d\varepsilon_{ij}^E = \frac{1}{E(T)}[(1+\nu(T))\,d\sigma_{ij} - \nu(T)\,\delta_{ij}d\sigma_{kk}] - \frac{1}{E^2(T)}[(1+\nu(T))\,\sigma_{ij} - \nu(T)\,\delta_{ij}\sigma_{kk}]\frac{\partial E(T)}{\partial T}dT + \frac{1}{E(T)}(\sigma_{ij} - \delta_{ij}\sigma_{kk})\frac{\partial \nu(T)}{\partial T}dT + \delta_{ij}\alpha(T)\,dT + \delta_{ij}T\frac{\partial \alpha(T)}{\partial T}dT; \tag{12}$$

$$d\varepsilon_{ij}^P = \frac{3}{2}\frac{\sigma_{ij} - \frac{1}{3}\sigma_{ij}\sigma_{kk}}{\sigma_i}\left(\frac{1}{E_s(T)} - \frac{1}{E(T)}\right)\left(d\sigma_i - \frac{d\sigma_T}{\partial T}dT\right); \tag{13}$$

$$d\varepsilon_{rr} = \frac{\partial}{\partial r}(du_r),\quad d\varepsilon_{\theta\theta} = \frac{du_r}{r}.$$

Here,

$$\sigma_i = \frac{1}{\sqrt{2}}\{(\sigma_{rr} - \sigma_{\theta\theta})^2 + (\sigma_{\theta\theta} - \sigma_{zz})^2 + (\sigma_{zz} - \sigma_{rr})^2\}^{1/2},$$

$$\varepsilon_i = \sqrt{\frac{3}{4}}\{(\varepsilon_{rr} - \varepsilon_{\theta\theta})^2 + (\varepsilon_{\theta\theta} - \varepsilon_{zz})^2 + (\varepsilon_{zz} - \varepsilon_{rr})^2\}^{1/2}, \tag{14}$$

$$\sigma_{kk} = \frac{1}{3}(\sigma_{rr} + \sigma_{\theta\theta} + \sigma_{zz}).$$

The value of $d\varepsilon_{zz}$ depends only on time, while the axial resultant is equal to zero:

$$\int_0^{R_2} d\sigma_{rr} r dr = 0. \tag{15}$$

It is assumed that the values of $\sigma_{ij}$, $\varepsilon_{ij}$, and $u_r$ are known at the initial instant of time and that the following conditions are satisfied at the boundaries: $du_r|_{r=0} = 0$, $[du_r]_{r=R_1} = 0$, $[d\sigma_{rr}]_{r=R_1} = 0$, and $d\sigma_{rr}|_{r=R_2} = 0$.

The nonlinear system (10)-(13) is solved for each time segment in the elastoplastic region by using the well-known method of additional strain [11]. Depending on the behavior of the temperature field, local return to the elastic region is possible. The criterion indicating that a purely elastic field is to be calculated consists of the following conditions that can be verified at each time step:

$$\sigma_i(\bar{\varepsilon}_i^P, T) < \sigma_T(\bar{\varepsilon}_i^P, T) \text{ or } \sigma_i(\bar{\varepsilon}_i^P, T) = \sigma_T(\bar{\varepsilon}_i^P, T),\ d\sigma_i < \left(\frac{d\sigma_T}{dT}\right)_{\bar{\varepsilon}_i^P} dT.$$

During the return to the elastic region, the plastic strain (if such has occurred) is memorized and is thus stored, along with the $\bar{\varepsilon}^P_i$ value.

The purely elastic fields are calculated by reducing system (10)-(15) for $d\varepsilon^P_{ij} = 0$ to the boundary-value problem for a system of two integrodifferential equations with respect to $du_r$ and $d\varepsilon_{zz}$, which is solved by using the difference trial-and-error method.

After finding the time increments of the sought quantities, we determine the values of the latter at the next (k-th) time segment in the obvious manner: $\sigma_{ij}^{(k)} = \sigma_{ij}^{(k-1)} + d\sigma_{ij}^{(k)}$, etc.

We shall now discuss the results of the mathematical experiment.

For one of the geometric configuration variants and an $\hat{f}$ value, Fig. 8 shows the distributions of the stress tensor components along the radius, in comparison with the temperature field distribution at different instants of time, corresponding to the maximum values of the stress drop in the outside layer of the bimetal.

According to the statement of the problem, $\sigma_{rr}$ is a continuous function of the radius, while $\sigma_{\theta\theta}$ and $\sigma_{zz}$ display discontinuities in view of the natural continuity of displacements at the interface between layers with different characteristics. The stress drop for any component, in particular, in the outside layer, does not exceed ~200 MPa (20 kg/mm$^2$).

Figure 9 provides the distribution of the stress field intensity as a function of time for another optimum control variant (see Fig. 4) in comparison with the yield point of the materials in the model chosen. The intensity $\sigma_i$ also has a discontinuity at the $r = R_1$ boundary.

It is evident that $\sigma_i$ nowhere exceeds ~230 MPa (23 kg/mm$^2$) and at no time exceeds the yield point in the outside layer. The core of the bimetal is at times in the plasticity region. However, after the heating ends, it also returns to the elastic state. This means that the residual stresses in the core cannot be large, while they are completely absent in the outside (operating) layer.

The corresponding characteristics of the stress field for the experimental variant (see Fig. 3) are shown in Fig. 10. The stress intensity in the outside layer is also in this case lower than the yield point for the material in question.

The stability of these results for sufficiently wide ranges of the parameters: 25 mm $\leq R_1 \leq$ 40 mm, 5 mm $\leq R_2 - R_1 \leq$ 10 mm, 50 Hz $\leq f_1 \leq$ 2400 Hz, and 500 Hz $\leq f_2 \leq$ 10,000 Hz, supports the expected correlation between the temperature field drop and the stress field and, thus, the validity of the statement of the optimization problem proposed above.

It should be mentioned that this problem can also be stated directly in terms of stresses. In this case, the above algorithm for calculating them constitutes the contents of the data unit program which uses the temperature field calculation unit. The stress intensity is considered as the functional of I: $\sigma_i = \sigma_i[r, t, I]$. In statement (9), the following can be assumed with an allowance for the jump of $\sigma_i$ at the interface:

Finally, either the value $\hat{\sigma}^2$, which limits the stress, or the function $\sigma_y^{0^2}(T)$ should be substituted for $\hat{\delta}^2$ in (9).

This statement of the problem is, however, less effective than the preceding one. Moreover, its use presupposes knowledge of all the mechanical characteristics of the material in question, which is not always the case [8]. In connection with this, it may prove useful to state inverse problems in a manner similar to that used for determining the current in section 3 and solve them by means of a certain regularizing algorithm.

## LITERATURE CITED


1. V. B. Glasko, L.A. Dubrovskaya, V. D. Kal'ner, et al., Method of Heating Bimetallic Steel Billets, Author's Certificate No. 1470783 [in Russian] (1989).
2. A. N. Tikhonov and V. Ya. Arsenin, Methods of Solving Improper Problems [in Russian], Moscow (1986).
3. V. B. Glasko, Inverse Problems of Mathematical Physics [in Russian], Moscow (1984).
4. A. N. Tikhonov, N. I. Kulik, I. N. Shklyarov, and V. B. Glasko, Inzh.-Fiz. Zh., 39, No. 1, 5-10 (1980).
5. A. N. Tikhonov and A. A. Samarskii, Equations of Mathematical Physics [in Russian], Moscow (1972).
6. A. A. Samarskii and E. S. Nikolaev, Methods for Solving Grid Equations [in Russian], Moscow (1978).
7. A. N. Tikhonov and V. B. Glasko, Zh. Vychisl. Mat. Mat. Fiz., 5, No. 3, 463-473 (1965).
8. V. S. Morganyuk, Probl. Prochn., No. 6, 80-85 (1982).
9. N. B. Vargaftik, Thermophysical Characteristics of Materials [in Russian], Moscow—Leningrad (1956).
10. A. A. Shmykov, Heat Specialist's Manual [in Russian], Moscow (1961).
11. I. A. Birger and B. F. Shor, Thermal Strength of Machine Parts [in Russian], Moscow (1975).


# THERMAL AND THERMODEFORMATIONAL PROCESSES IN THE FORCED HEATING OF STEEL


**Yu. A. Malevich, V. N. Papkovich, P. V. Sevast'yanov, D. G. Sedyako, and L. G. Dymova**



UDC 621.785



*The dynamics of metal heating in a furnace of pacing-beam type is investigated experimentally and theoretically.*


The heating of metal in a furnace is investigated experimentally, with the aim of subsequent parametric identification of the mathematical model, for the example of steel-15 blooms of cross section 250 × 300 mm.

In the course of the industrial experiment, the temperature values of control points of the cross section of the experimental ingot (corner, surface, center) is determined from the instant of insertion to the removal of the metal, as well as the degree of oxidation of surface layers of the steel. The temperature is measured using KhA thermocouples with an electrode diameter of 1.2 mm. The productivity of the heating furnace in the experiment is 46.7 ton/h.

Note that the presence of a positive static pressure in the working space of the furnace eliminates the possibility of cold-air inflow. Ignition of the fuel with a consumption coefficient of 1.0-1.1 in these conditions creates an atmosphere with weak oxidative properties. This is confirmed by the experimental results: the degree of oxidation of the metal is no more than 1%.

Analysis of the components of the thermal balance allows the efficiency of the furnace and the specific consumption of the conventional fuel to be determined: 61.5% and 35.2 kg of fuel/ton of steel, respectively. The total heat losses through the load with cooling water and with incomplete chemical combustion are no more than 10%, which indicates high efficiency of operation of the furnace.


Belorussian Polytechnic Institute, Minsk. Mogilevsk Branch, Physicotechnical Institute, Academy of Sciences of the Belorussian SSR.


Translated from Inzhenerno-Fizicheskii Zhurnal, Vol. 58, No. 3, pp. 402-405, March, 1990. Original article submitted February 6, 1989.



0022-0841/90/5803-0289$12.50